LPV-MPC Path Planner for Autonomous Underwater Vehicles

Luca Cavanini *, **Pawel Majecki** *, **Mike J. Grimble** *, **Hiroshi Uchihori** **, **Mitsuhiko Tasaki** ** **Ikuo Yamamoto** ***

* *Industrial Systems and Control, Ltd, Culzean House, 36 Renfield Street, Glasgow G2 1LU, UK (e-mail: {l.cavanini, pawel, m.grimble}@isc-ltd.com)*
** *Mitsubishi Heavy Industries, Ltd, 6-53 Tsukuba-machi, Isahaya City, Nagasaki, 854-0065 Japan (e-mail: {hiroshi_uchihori, mitsuhiko_tasaki}@mhi.co.jp)*
*** *Nagasaki University, 1-14 Bunkyo-machi, Nagasaki City, Nagasaki 852-8521, Japan (e-mail: iyamamoto@nagasaki-u.ac.jp)*

Abstract: A path planning algorithm for an Autonomous Underwater Vehicle (AUV) performing docking operations in the presence of tidal current disturbances is presented. The path planner is composed a way-point generator (WPG), an Model Predictive Control based optimal planner (OP), and a tidal current estimator (TCE). The WPG defines the next way-point with respect to the vehicle position and the OP iteratively generates the trajectory over a prescribed future horizon whilst satisfying certain physical and logical constraints. The TCE estimates the tidal current disturbance speed enabling to adapt the AUV trajectory for reducing actuators power consumption. The proposed path planning policy has been evaluated in a set of simulation scenarios to illustrate the ability of the policy to drive the AUV by satisfying specifications and limiting power consumption.

Keywords: Path Planning, Model Predictive Control, Autonomous Underwater Vehicle

1. INTRODUCTION

Autonomous Underwater Vehicles (AUVs) are submarine robotic systems widely used in marine applications for oceanographic research, submarine oil pipe status monitoring and ecological observations (Antonelli et al. (2016)). A wide set of different situations can be handled by AUVs due to their ability to explore the marine environment and perform tasks with a high degree of autonomy and robustness (Alvarez et al. (2004)). In the following, a path planning algorithm for an AUV will be presented. The trajectory generation is a widely studied problem in autonomous robotics and in AUV control. Several methods have been proposed in the past to address AUV path planning issues, e.g. reducing travel time (Alvarez et al. (2004)) by different paradigms such as optimal control (Cavanini and Ippoliti (2018)) or Artificial Intelligence (Zhu et al. (2017)) customized to address specific features of AUV path planning problems. In this paper, a path planner based on Model-based Predictive Control (MPC) is proposed. The algorithm is composed of three different elements. The first module is a Way-Points Generator (WPG) that computes future vehicle reference positions over the control scenario with respect to measurements of vessel and the docking station poses. The second component is an MPC-based trajectory generator denoted the Optimal Planner (OP) which iteratively computes the vehicle trajectory between way-points. This MPC is based on a Linear Parameter-Varying (LPV) design model representing the closed-loop system given by AUV and tracking controller. The last module is the Tidal Current Estimator (TCE), which estimates the underwater current velocities. The estimation is needed for adapting the OP trajectory. The policy has been tested in simulations validating the capability to adapt the vehicle's trajectory to different tidal current velocities. The paper presents the vehicle model in Section 2, the path planning problem and controller in Section 3, the simulation results in Section 4, and conclusions in Section 5.

⋆ This research was funded by Nippon Foundation, grant number 'UYSjgc9y'.

2. AUV MODELLING

2.1 Rigid-body Dynamics Model

The AUV dynamics are defined by a set of nonlinear equations with respect to two reference frames termed the Earth-Fixed (Inertial) used to represent the vehicle pose (position and orientation) and Body-Fixed frames used for (linear and angular) velocities and coincident with the AUV center of buoyancy, as shown in Figure 1. The notation from the Society of Naval Architects and Marine Engineers (SNAME) is considered (Lewis (1988)) such that AUV velocities are $\nu = [u, v, w, p, q, r]^T$, with $\nu_1 = [u, v, w]^T$ linear surge, sway and heave velocity and $\nu_2 = [p, q, r]^T$ angular roll, pitch and yaw speed, and positions are $\eta = [x, y, z, \phi, \theta, \psi]^T$ with $\eta_1 = [x, y, z]^T$ linear position and $\eta_2 = [\phi, \theta, psi]^T$ the angular orientation, such that $\dot{\eta}_1 = J_1(\eta_2)\nu_1$, $\dot{\eta}_2 = J_2(\eta_2)\nu_2$ with

$$J_1(\eta_2) = \begin{bmatrix} c(\psi)c(\theta) & -s(\psi)c(\phi) + c(\psi)s(\theta)s(phi) & s(\psi)s(\psi) + c(\psi)c(\phi)s(\theta) \\ s(\psi)c(\theta) & c(\psi)c(\phi) + s(\phi)s(\theta)s(phi) & c(\psi)s(phi) + s(\theta)s(\psi)c(\phi) \\ -s(\theta) & c(\theta)s(\phi) & c(\theta)c(2phi) \end{bmatrix} \quad (1)$$

$$J_2(\eta_2) = \begin{bmatrix} 1 & t(\theta)s(\phi) & t(\theta)c(\phi) \\ 0 & c(\phi) & -s(\phi) \\ 0 & \frac{s(\phi)}{c(\theta)} & \frac{c(\phi)}{c(\theta)} \end{bmatrix} \quad (2)$$

where $s(\alpha) = \sin(\alpha)$, $c(\alpha) = \cos(\alpha)$ and $t(\alpha) = \tan(\alpha)$. Eqs.(1)-(2) can be written in a compact form such that $\eta = J(\eta_2)\nu$ with $J(\eta) = diag(J_1(\eta_2), J_2(\eta_2)$. AUV equations

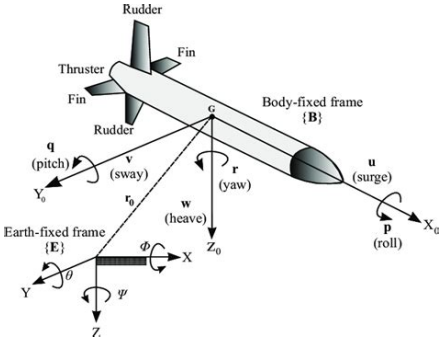

Fig. 1. Reference frames for the AUV model from Alvarez et al. (2004)

of motion involve the rigid–body dynamic terms and components related to hydrodynamic forces and moments. These are modeled considering restoring forces, added mass and damping. The AUV nonlinear dynamic model is formulated in a matrix form (Antonelli et al. (2016)) such that :

$$M\dot{\nu} + C(\nu)\nu + D(\nu)\nu + g(\eta) = \tau_A \quad (3)$$

where $M = M_{RB} + M_{AM}$ is the rigid-body mass matrix with M_{RB} the constant rigid-body inertia matrix and M_{AM} the added inertia matrix, $C(\nu) = C_{RB}(\nu) + C_{AM}(\nu)$ is the matrix of Coriolis and centripetal terms, with with $C_{RB}(\nu)$ representing the constant mass and $C_{AM}(\nu)$ the centripetal and Coriolis added mass effects, the term $g(\eta) = [X_R, Y_R, Z_R, K_R, M_R, N_R]^T$ is the vector of restoring forces and moments, $D(\nu)$ represents damping phenomena that are modeled as a function of instantaneous vehicle velocities ν, and $\tau_a = [X, Y, Z, K, M, N]^T$ is the vector of external forces (X, Y, Z) and moments (K, M, N) acting on the vehicle (e.g. effect of actuators). The vehicle is subject to underwater currents that need countering and are described by the speed components $\nu_T = [u_T, v_T, w_T, p_T, q_T, r_T]^T$ such that the relative velocity of the vehicle with respect to the tidal current can be computed by $\nu_R = \nu - \nu_T$. The effect of the current is then included in the rigid-body dynamics model of Eq.(3) by replacing ν with ν_R so that:

$$M\dot{\nu_R} + C(\nu_R)\nu_R + D(\nu_R)\nu_R + g(\eta) = \tau_A. \quad (4)$$

Remark 1. *The tidal current ν_T is assumed constant in direction and velocity $(\dot{u}_T = \dot{v}_T = \dot{w}_T) = 0$ $[m/s]$), irrotational $(p_T = q_T = r_T = 0[m/s])$ and the vertical component of the current is negligible $(w_T = 0[m/s])$.*

Remark 2. *According to the specifications describing the control scenario, the tidal current speed $V_T = \sqrt{u_T^2 + v_T^2}$ is bounded such that $V_T \in [0, 0.514]$ $[m/s]$.*

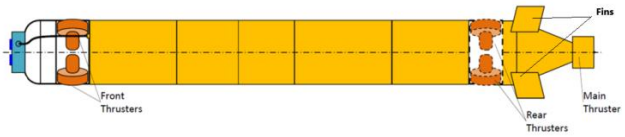

Fig. 2. AUV Layout

Remark 3. *The constant tidal current heading orientation is $\psi_T = \psi_{ROV} + \beta$ where ψ_{ROV} is the docking station heading and $\beta \in [-0.1745, +0.1745]$ rad is a constant term representing different control scenarios.*

2.2 Actuators and Sensors

The AUV is equipped with a set of actuators including fins and thrusters mounted in different positions over the vehicle hull, as shown in Figure 2. The actuators are the main thruster, side thrusters (front and rear), and fins (stern planes and rudders) and are characterized as in the following sections.

The main thruster is positioned at the stern of the vehicle, aligned with the x-axis of the Body-Fixed reference frame and cannot provide forces or moments other than the force over this axis. The force generated by this thruster follows this relationship:

$$X_M = k_t(J)\rho n^2 D_0^4 \frac{\omega_n^2}{s^2 + 2s\omega_n\zeta + \omega N^2} \quad (5)$$

where $\rho = 1024\ kg/m^3$ is the water density, $u_M = n$ [rpm] is the control input (the required rotation speed), $D_0 = 0.152$ m is the nominal thruster diameter, $k_t(J)$ represents the nonlinear relationship between actual speed and control input such that:

$$k_t(J) = -0.46J + 0.66 \quad \text{if} \quad J > 0 \quad (6)$$

$$k_t(J) = -0.46J \quad \text{if} \quad J < 0 \quad (7)$$

where $J = u_r/(nD_0)$, and u_r $[m/s]$ is the vehicle forward speed with respect to water, s is the Laplace variable, $\omega_n = 1$ Hz is the natural frequency of the second-order actuator dynamic system and $\zeta = 1.5$ is the damping factor. The main thruster dynamics is featured by two nonlinerities relating to saturation $(+/-2000$ [rpm]) and dead zone $(+/-400$ [rpm]) in the control input channel.

Fins are located at the end of the vehicle, near the main thruster. Their dynamics is directly related to the vehicle pose and velocities, according to a set of relationships determined by the fins' lift coefficients. The force and moment provided by the rudder fins (Y_r and N_r), stern planes (Z_s and M_s) and their combined effect (K_{rs}) are:

$$Y_r = 0.5Y_{uu\delta r}(u^2 0.5\delta_{r1} + u^2 0.5\delta_{r2} - uv) + 0.5Y_{urf}ur \quad (8)$$

$$Z_s = 0.5Z_{uu\delta s}(u^2 0.5\delta_{s1} + u^2 0.5\delta_{s2} - uw) + 0.5Y_{urf}uq \quad (9)$$

$$K_{rs} = 0.5K_{uu\delta r}(0.5\delta_{r1} - 0.5\delta_{r2} + 0.5\delta_{s1}0.5\delta_{s2}) \quad (10)$$

$$M_s = 0.5Y_{uu\delta s}(u^2 0.5\delta_{s1} + u^2 0.5\delta_{s2} - uw) + 0.5M_{uqf}uq \quad (11)$$

$$N_r = 0.5N_{uu\delta r}(u^2 0.5\delta_{r1} + u^2 0.5\delta_{r2} - uv) + 0.5M_{uqf}ur \quad (12)$$

The fins control input is the deviation angle respect to the zero position ($\delta_{r1,2}$ and $\delta_{s1,2}$ for rudders and stern-planes, respectively), and it is subject to saturation at maximum/minimum values (± 30 degrees) according to system specifications. The dynamics of the fins' angular position response is modelled by a second-order system with a natural frequency $\omega_n = 4$ Hz and a damping factor $\zeta = 0.7$. Side thrusters are placed on the side of the vehicle's hull to drive the AUV at low speeds when

the forward speed of the vehicle is too low for the fins to provide an effective control action. The effort provided by each side thruster can be split into two components such that the combination of thrusters' efforts may be modeled by the following relationships:

$$\tau_{ST} = \begin{bmatrix} 0 & 0 & 0 & 0 \\ -c(\alpha) & -c(\alpha) & c(\alpha) & c(\alpha) \\ -c(\alpha) & -c(\alpha) & c(\alpha) & c(\alpha) \\ -d & d & -d & d \\ D_F c(\alpha) & -D_F c(\alpha) & -D_F c(\alpha) & D_F c(\alpha) \\ -D_F c(\alpha) & -D_F c(\alpha) & D_F c(\alpha) & D_F c(\alpha) \end{bmatrix}$$

$$\begin{bmatrix} 0 & 0 & 0 & 0 \\ -c(\alpha) & -c(\alpha) & c(\alpha) & c(\alpha) \\ -c(\alpha) & -c(\alpha) & c(\alpha) & c(\alpha) \\ -d & d & -d & d \\ -D_F c(\alpha) & D_F c(\alpha) & D_F c(\alpha) & -D_F c(\alpha) \\ D_F c(\alpha) & D_F c(\alpha) & -D_F c(\alpha) & -D_F c(\alpha) \end{bmatrix} \begin{bmatrix} F_{F1} \\ F_{F2} \\ F_{F3} \\ F_{F4} \\ F_{R1} \\ F_{R2} \\ F_{R3} \\ F_{R4} \end{bmatrix} \quad (13)$$

with $\tau_{ST} = [X_{ST}, Y_{ST}, Z_{ST}, N_{ST}, M_{ST}, N_{ST}]^T$, where $c(\alpha) = \cos(\alpha)$ and $\alpha = 45$ degrees is the angular position of thrusters (for $\alpha = 45$ degrees $\sin(\alpha) = \cos(\alpha)$) and τ_{ST} is the vector of forces and moments provided by side thrusters. The force provided by each side thruster is given by actuator nonlinear characteristic, converting the PWM duty-cycle (from the Attitude controller) to the thruster effort. These thrusters also include a saturation on the maximum force and a symmetric dead-band centered on the zero speed (equivalent to $1500\mu s$ PWM input signal) and a delay of 0.01875 s and has the following dynamic model:

$$A_T = \begin{bmatrix} -10^{-3} & -25 \times 10^4 \\ 1 & 0 \end{bmatrix}; B_T = \begin{bmatrix} 1 \\ 0 \end{bmatrix}; C_T = \begin{bmatrix} 0 & 25 \times 10^4 \end{bmatrix}. \quad (14)$$

The thrust $y_T = T$ [N] provided by each thruster is defined in terms of the control input signal u_T =PWM [ms] and $y_T(k) = a_2(k)u_T^2(k) + a_1(k)u_T(k) + a_0(k)$ such that:

- If $u_T(k) > 1.5381$ then $a_2(k) = 54.262$, $a_1(k) = -108.231$ and $a_0(k) = 38.101$;
- If $u_T(k) < 1.4492$ then $a_2(k) = -28.058$, $a_1(k) = 134.08$ and $a_0(k) = -135.38$;
- If $u_T(k) \in [1.4492, 1.5381]$ then $a_2(k) = 0$, $a_1(k) = 0$ and $a_0(k) = 0$.

The AUV is equipped with a set of sensors to measure position and orientation of the vehicle with respect to the inertial reference frame, and linear and angular velocities with respect to the Body-Fixed reference frame. A delay of 20 ms affects sensors' measurements. The accuracy of the linear position sensors is 0.005 m and the linear velocities accuracy is 0.1 m/s. The angular position measurements have an accuracy of 5.42×10^{-5} rads, and the angular velocities accuracy is 5.42×10^{-3} rad/s.

2.3 Attitude Control System

The Attitude control system represents the low-level controller in the AUV, aided to track reference signals provided by the path planner. The design of this control layer is out of the scope of the paper and would be developed according to different control paradigms widely applied in the underwater control field, e.g. MPC (Medagoda and Williams (2012)) or Gain-scheduling control (Silvestre and Pascoal (2007)). In this work, the attitude controller would track vehicle forward speed reference signal u_r and the heading reference ψ_r defined by the path planner, such that the path planning problem considers the trajectory only over the x-y plane.

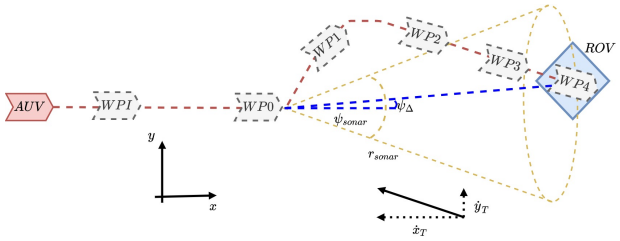

Fig. 3. AUV Control Scenario: the AUV trajectory on the x-y plane with respect to way-points, ROV position, sonar range, x-y axis representing the inertial reference frame and tidal current components $\dot{x}_T$, $\dot{y}_T$.

3. AUV PATH PLANNER

This AUV application involves a vehicle that autonomously moves through a set of way-points to approach a prescribed final position, where it can be caught by the Remotely Operated Vehicle (ROV) docking station. A way-point defines the vehicle position (over x,y axes) and orientation (ψ angle), and also provides information about the maximum forward velocity u_{WP}^{MAX} to be maintained whilst approaching the docking position. Other linear and angular positions are considered constant (zero). A simplified control scenario showing different way-points is presented in Figure 3 The trajectory to be followed by the AUV (and computed by the OP) is shown by a dashed red line. The position of the ROV with respect to the WP0 is defined by the angle ψ_Δ, whereas the sonar range of vision is defined by the sonar angular range ψ_{sonar} and the related maximum range r_{sonar}. Also an unmeasurable tidal current affects the vehicle dynamics as presented in Eq. (4).

3.1 Path Planning Policy

The proposed approach involves several functional modules structured as shown in Figure 4. The path planning policy (yellow box) drives the closed-loop system (blue box) which represents the AUV (green block) driven by the attitude controller (purple block). The path planner is composed of a WPG, an OP, and a TCE. The policy uses the measurement of the AUV output signals $y_{AUV} = [x, y, z, \phi, \theta, \psi, u, v, w, p, q, r]^T$. The WPG uses measured AUV position to define the next way-point signal $r_{WP} = [\bar{x}_r, \bar{y}_r r, \bar{\psi}_r]^T$ and the maximum forward speed u_{WP}^{MAX}. The OP computes the future vehicle trajectory (x_r, y_r) and the control signals to be tracked by the attitude controller $r_{AUV} = [\psi_r, u_r]^T$. The TCE uses the measured vehicle output signal y_{AUV} and the control signals generated by

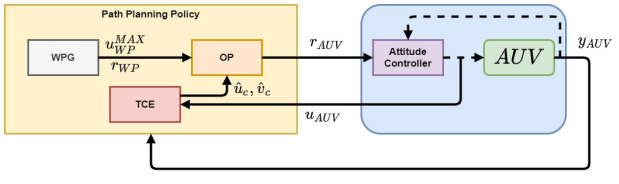

Fig. 4. AUV Path Planning Policy Architecture

Algorithm 1 Way-points Generator Algorithm

Input: x-axis AUV position $x(k)$, y-axis AUV position $y(k)$ at the k-th time instant

1: **if** $x(k) < x_{SWPI}$ **then**
2: $r_{WP} \leftarrow \mathrm{r}_{WP0}$, $u_{WP}^{MAX} \leftarrow \mathrm{u}_{WP}^{0}$
3: **else if** $x(k) < x_{SWP0}$ & $x(k) > x_{SWPI}$ **then**
4: $r_{WP} \leftarrow \mathrm{r}_{WP1}$, $u_{WP}^{MAX} \leftarrow \mathrm{u}_{WP}^{1}$
5: **else if** $x(k) < x_{SWP1}$ & $x(k) > x_{SWP0}$ **then**
6: $r_{WP} \leftarrow \mathrm{r}_{WP2}$, $u_{WP}^{MAX} \leftarrow \mathrm{u}_{WP}^{2}$
7: **else if** $x(k) < x_{SWP2}$ & $x(k) > x_{SWP1}$ **then**
8: $r_{WP} \leftarrow \mathrm{r}_{WP3}$, $u_{WP}^{MAX} \leftarrow \mathrm{u}_{WP}^{3}$
9: **else if** $r \geq \sqrt{(x(k) - x_{SWP2})^2 + (y(k) - y_{SWP2})^2}$ **then**
10: $r_{WP} \leftarrow \mathrm{r}_{WP4}$, $u_{WP}^{MAX} \leftarrow \mathrm{u}_{WP}^{4}$
11: **end if**

Output: next way-point value $r_{WP}(k)$ and maximum forward speed u_{WP}^{MAX} at the k-th time instant.

the attitude controller $u_{AUV} = [\ u_M,\ \delta_{r1},\ \delta_{r2},\ \delta_{s1},\ \delta_{s2},\ u_{SF1},\ u_{SF2},\ u_{SF3},\ u_{SF4},\ u_{SR1},\ u_{SR2},\ u_{SR3},\ u_{SR4}\ ]^T$ for estimating tidal current velocities $\hat{u}_T$, $\hat{v}_T$. The estimate tidal current speed is used within the OP.

3.2 Way-points Generator

The WPG provides maximum forward speed and poses for representing the next way-point to be reached by the AUV and the policy is defined as in Algorithm 1: operations 1-8 enable one to evaluate if the vehicle is between two way-points, whereas the last operations 9-10 is used to verify if the AUV is within the circle of acceptance of radius r and centered on the final docking station position. The WPG parameters are computed as in Table 1. In WP3 the vehicle is decelerating and the maximum forward speed decreases while approaching the docking station such that the AUV will stop in this position waiting for the ROV.

3.3 Optimal Planner

The OP has been formulated according to the MPC framework. The closed-loop system composed of AUV and attitude controller is modelled as a unicycle moving over the x-y plane. This system is described by a LPV discrete-time state-space model

$$\mathrm{x}_{k+1} = \underbrace{\begin{bmatrix} 1 & 0 & 0 \\ 0 & 1 & 0 \\ 0 & 0 & 0 \end{bmatrix}}_{A} \mathrm{x}_k + \underbrace{\begin{bmatrix} T_s\cos(\psi(k)) & 0 \\ T_s\sin(\psi(k)) & 0 \\ 0 & 1 \end{bmatrix}}_{B_k} \mathrm{u}_k \ ;\ \mathrm{y}_k = \underbrace{\begin{bmatrix} 1 & 0 & 0 \\ 0 & 1 & 0 \\ 0 & 0 & 1 \end{bmatrix}}_{C} \mathrm{x}_k \tag{15}$$

where $\mathrm{x}_k = [x(k), y(k), \psi(k)]^T$ is the state vector representing actual AUV position and orientation, $\mathrm{y}_k = \mathrm{x}_k$ is the output vector, $\mathrm{u}_k = [u_r(k), \psi_r(k)]^T$ is the control input driving the closed-loop system and the state-space matrices are featured by scheduling parameters defined by vehicle orientation at the k-th time instance $\psi(k)$ and the controller sampling time T_s. To adapt the trajectory of the vehicle to the instantaneous pose of the AUV, uncertain environment and current disturbances, the vessel should be able to change the heading angle. The instantaneous heading reference angle enabling to compute the minimum length path to the next way-point is reference heading angle $\bar{\psi}_r(k)$ for the OP, such that as in Table 1:

$$\bar{\psi}_r = \arctan \frac{\bar{y}_r - y(k)}{\bar{x}_r - x(k)} \tag{16}$$

where $(\bar{x}_r(k), \bar{y}_r(k))$ is the next way-point position provided by WPG, $r(k) = [\bar{x}_r(k), \bar{y}_r(k)\bar{\psi}_r(k)]^T$ is the reference vector, and $(x(k), y(k))$ is current position of the vehicle. Among different possibilities (Zeng et al. (2015), Albarakati et al. (2019)), in the considered approach the reference heading angle $\bar{\psi}_r(k)$ is adapted by using the estimated current velocities $\hat{\dot{x}}_c(k), \hat{\dot{y}}_c(k)$ acting on the vehicle. The proposed approach considers that the main thruster should always be active and would be used to maintain the vehicle speed also in the presence of tidal current whereas side thrusters should be used less to limit lateral displacement. Because the main effect of the current is to move the vehicle laterally, the control policy tends to set the lateral speed of the vehicle to zero, such that

$$\dot{y}(k) + \hat{\dot{y}}_c(k) = 0 \tag{17}$$

where $\dot{y}(k)$ is the lateral speed of the vehicle when the current speed is zero and $\hat{\dot{y}}_c(k)$ is the tidal current velocity. Eq.(17) can be formulated in terms of the vehicle forward speed $u(k)$, heading angle $\psi(k)$ and correction angle $\psi_{co}(k)$ to be included in the heading angle such that the angle $\bar{\psi}_r(k) + \psi_{co}(k)$ is the angle to be followed by the vehicle in the opposite direction of the current:

$$u(k)\sin(\bar{\psi}_r(k) + \psi_{co}(k)) + \hat{\dot{y}}_c(k) = 0. \tag{18}$$

The angular correction $\psi_{co}(k)$ should be iteratively evaluated based on the above condition. By applying trigonometric relations, the above equation can be written as:

$$u(k)(\sin(\bar{\psi}_r(k))\cos(\psi_{co}(k)) + \cos(\bar{\psi}_r(k))\sin(\psi_{co}(k))) + \hat{\dot{y}}_c(k) = 0 \tag{19}$$

and further manipulated as

$$u(k)\frac{\sin(\bar{\psi}_r(k))}{\cos(\bar{\psi}_r(k))}\cos(\psi_{\Delta}(k)) + u(k)\sin(\psi_{co}(k) = -\frac{\hat{\dot{y}}_c(k)}{\cos(\bar{\psi}_r(k))} \tag{20}$$

Table 1. Way-points Values and Parameters

Parameter	Value
Positions	$x_{SWPI} = x_0 - (x_{sonar} - r_{sonar})$
	$y_{SWPI} = 0$
	$x_{SWP0} = 0$, $x_{SWP0} = 0$
	$x_{SWP1} = x_{SWP2} - r_{sonar}\cos(\psi_{ROV})$
	$y_{SWP1} = x_{SWP2} + r_{sonar}\sin(\psi_{ROV})$
	(x_{SWP2}, y_{SWP2}) =docking position
WP0	$r_{WP0} = [\bar{x}_r, \bar{y}_r, \bar{\psi}_r]^T$
	$\bar{x}_r = x_{SWPI}$, $\bar{y}_r = y_{SWPI}$
	$\bar{\psi}_r = 0$, $u_{WP}^{0} = 2.056$ [m/s]
WP1	$r_{WP1} = [\bar{x}_r, \bar{y}_r, \bar{\psi}_r]^T$
	$\bar{x}_r = x_{SWP1}$, $\bar{y}_r = y_{SWP1}$
	$\bar{\psi}_r = 0$, $u_{WP}^{1} = 1.028$ [m/s]
WP2	$r_{WP2} = [\bar{x}_r, \bar{y}_r, \bar{\psi}_r]^T$
	$\bar{x}_r = 0.5(x_{SWP1} - x_{SWP2}) + x_{SWP1}$
	$\bar{y}_r = 0.5(y_{SWP1} - y_{SWP2}) + y_{SWP1}$
	$u_{WP}^{2} = 1.028$
	$\bar{\psi}_r = \arctan \frac{y_r - y(k)}{x_r - x(k)}$
WP3	$r_{WP3} = [\bar{x}_r, \bar{y}_r, \bar{\psi}_r]^T$
	$\bar{x}_r = x_{SWP2}$, $\bar{y}_r = y_{SWP2}$
	$\bar{\psi}_r = \arctan \frac{y_{SWP2} - y(k)}{x_{SWP2} - x(k)}$
	$u_{WP}^{1} = 1.028 - \dot{u}\Delta T$ with $\dot{u} = -\frac{\bar{u}_r}{T}$
	$T = \frac{2\Delta}{u_r}$, $\Delta = \sqrt{(x_k - \bar{x}_r)^2 + (y_k - \bar{y}_r)^2}$
WP4	$r_{WP4} = [\bar{x}_r, \bar{y}_r, \bar{\psi}_r]^T$
	$\bar{x}_r = x_{SWP2}$, $\bar{y}_r = y_{SWP2}$, $\bar{\psi}_r = \psi_{SWP2}$

such that

$$\tan(\bar{\psi}_r(k))\cos(\psi_\Delta(k)) + \sin(\psi_\Delta(k)) = -\frac{\hat{y}_c(k)}{u(k)\cos(\bar{\psi}_r(k))}. \quad (21)$$

Consider the trigonometric functions Taylor-Maclaurin series expansion approximated at the first term, Eq.(21) becomes

$$\tan(\bar{\psi}_r(k)) + \psi_{co}(k) = -\frac{\hat{y}_c(k)}{u(k)\cos(\bar{\psi}_r(k))} \quad (22)$$

such that the correction angle is

$$\psi_{co}(k) = -\frac{\hat{y}_c(k)}{u(k)\cos(\bar{\psi}_r(k))} - \tan(\bar{\psi}_r(k)). \quad (23)$$

This policy iteratively adapts the heading reference to be tracked, so that it is smoothly changed with the vehicle's position. Further, the trajectory will guarantee that the vehicle would maintain the ROV within the cone of vision of AUV sensors. This is included by reference heading angle constraints:

$$\psi_r^{min}(k+i) \leq \psi_r(k+i) \leq \psi_r^{MAX}(k+i) \quad (24)$$

where

$$\psi_r^{min}(k+i) = \arctan\frac{\bar{y}_r - y_N(k)}{\bar{x}_r - x_N(k)} - \psi_{sonar} \quad (25)$$

$$\psi_r^{MAX}(k+i) = \arctan\frac{\bar{y}_r - y_N(k)}{\bar{x}_r - x_N(k)} + \psi_{sonar} \quad (26)$$

with ψ_{sonar} the maximum angle defining the cone of vision of AUV sensors and (x_N, y_N) is the position of the nose (sonar) of the vehicle. Further, to limit the side thrusters' power consumption, the predictive control paradigm used in the OP includes control action rate limits, so that:

$$\psi_r(k+i) - \Delta\psi^m \leq \psi_r(k+i+1) \leq \psi_r(k+i) + \Delta\psi^M \quad (27)$$

where $\psi_r(k+i+1)$ is the predicted heading angle reference signals computed by the OP at the $(k+i+1)$-th time instant, $\psi_r(k+i)$ is the reference signal computed at the $(k+i)$-th time instant and $\Delta\psi^m, \Delta\psi^M$ are the minimum and maximum control signal rates that can be treated as calibration parameters for the OP policy. Considering the LPV model of Eq.(15), the set of reference signals and constraints to be satisfied when computing a smooth trajectory, the Optimal Path policy can be obtained by solving the following LPV-MPC problem:

$$\begin{aligned}
\min_{\Delta u} \quad & \sum_{i=1}^{N_p-1} \|Q(\mathrm{y}(k+i|k) - \mathrm{r}(k))\|_2^2 + \sum_{j=1}^{N_u} \|R\Delta\mathrm{u}(k+j|k)\|_2^2 \\
& + \|P(\mathrm{y}(k+N_p|k) - \mathrm{r}(k+N_p))\|_2^2 && (28a)\\
\text{s.t.} \quad & \mathrm{x}(k+i+1|k) = A\mathrm{x}(k+i|k) + B(k)\mathrm{u}(k+i) && (28b)\\
& \mathrm{y}(k+i|k) = C\mathrm{x}(k+i|k) && (28c)\\
& \mathrm{x}(k|k) = \hat{\mathrm{x}}(k) && (28d)\\
& \mathrm{u}(k+1+i) = \mathrm{u}(k+1) \ \text{ for } \ i > N_u && (28e)\\
& \mathrm{u}(k+1+i) = \mathrm{u}(k+1) + \Delta\mathrm{u}(k+1+i) \text{ for } i \leq N_u && (28f)\\
& \Delta\mathrm{u}(k+i) \in \mathbb{D} && (28g)\\
& \mathrm{u}(k+i) \in \mathbb{U} && (28h)\\
& \mathrm{y}(k+i) \in \mathbb{Y} && (28i)\\
& N_p \geq N_u && (28j)
\end{aligned}$$

with Q, R and P matrices for weighting the predicted output error, input-rate and final output value (terminal weight) respectively, $\mathrm{y}(k+i|k)$ the output predicted i steps ahead, $\mathrm{r}(k)$ the reference output assumed constant over the prediction/control horizon, $\Delta\mathrm{u}(k+j|k)$ and $\mathrm{u}(k+j|k)$ the predicted input rate and input magnitude respectively, N_p the prediction horizon, N_u the control horizon, $\mathbb{D}$ the convex set on input rate limits, and $\mathbb{U}$ and $\mathbb{Y}$ convex sets on control input magnitude and controlled output magnitude constraints. The LPV paradigm enables to formulate the MPC-based OP problem by a Quadratic Programming (QP) form suitable for real-time computation:

$$\begin{aligned}
\min_{\mathrm{z}} \quad & \frac{1}{2}\mathrm{z}'H_k\mathrm{z} + \rho_k'F_k'\mathrm{z} \\
\text{s.t.} \quad & G_k\mathrm{z} \leq h_k\rho_k + \mathrm{w}_k
\end{aligned} \quad (29)$$

where z is the vector of optimization variables, ρ_k is the vector of MPC parameters belonging to a given set, H_k is a symmetric and positive definite matrix, F_k is the linear cost term matrix and G_k, h_k and w_k are the terms defining constraints on the inputs and outputs.

3.4 Tidal Current Estimator

The tidal current estimator exploits the time-varying Kalman Filter (KF) framework (Grimble (2006)) to estimate unmeasurable tidal velocities by extending the state-vector to include the unknown variables representing the tidal current speed acting on the vehicle over the x and y axes:

$$\begin{aligned}
& \hat{\mathrm{x}}_F(k+1|k) = \hat{\mathrm{x}}_F(k|k) + M(k)\left(\mathrm{y}_F(k) - C_F(k)\hat{\mathrm{x}}_F(k|k-1)\right)\\
& M(k) = P(k|k-1)C_F^T(k)\left(C_F(k)P(k|k-1)C_F^T(k) + R_F\right)\\
& P(k|k) = (I - M(k)C_F(k)P(k|k-1))\\
& \hat{\mathrm{x}}_F(k+1|k) = A_F(k)\hat{\mathrm{x}}_F(k|k) + B_F(k)(u)_F(k) + d_F(k)\\
& P(k+1|k) = A_F(k)P(k|k)A_F^T(k) + B_F(k)Q_FB_F^T(k)
\end{aligned} \quad (30)$$

where Q_F and R_F are the disturbance and measurement covariance matrices and $A_F(k)$, $B_F(k)$, $C_F(k)$ and $d_F(k)$ are LPV discrete-time matrices of the AUV model in state-space form, derived from the following continuous-time matrices:

$$A_F(t) = \begin{bmatrix} \bar{A}(t) & a_{u_c}(t) & a_{v_c}(t) & a_{w_c}(t) \\ 0_{3\times6} & 0_{3\times1} & 0_{3\times1} & 0_{3\times1} \end{bmatrix}, B_F(t) = \begin{bmatrix} M^-1 \\ 0_{3\times6} \end{bmatrix} \quad (31)$$

$$C_F = \begin{bmatrix} I_{6\times6} & 0_{6\times3} \end{bmatrix}, d_F(t) = \begin{bmatrix} -M^-1g(\eta(t)) \\ 0_{3\times1} \end{bmatrix}. \quad (32)$$

These are defined by vehicle dynamics model, such that $\bar{A}(t) = [-M^{-1}(C(\nu(t)) + D(\nu(t))]$ and terms a_{u_c}, a_{v_c}, a_{w_c} are the first, second and third columns of the matrix $\bar{A}(t)$, respectively. Estimated variables are current speed with respect to forward vehicle speed $u_c(k)$ direction and lateral vehicle speed $v_c(k)$ direction. The estimated state-space vector for the KF-based current estimator is $\hat{\mathrm{x}}_F(k) = [\hat{u}(k), \hat{v}(k), \hat{w}(k),\ \hat{p}(k), \hat{q}(k), \hat{r}(k), \hat{u}_c(k), \hat{v}_c(k), \hat{w}_c(k)]$ where $u_c(k)$, $\hat{v}_c(k)$ and $\hat{w}_c(k)$ are estimated linear velocities $\hat{p}(k)$,$\hat{q}(k)$ and $\hat{r}(k)$ are estimated angular velocities, and $\hat{u}(k)$, $\hat{v}(k)$ and $\hat{w}(k)$ are estimated tidal current velocities. The final output of this estimator includes $\hat{u}_c(k)$ and $\hat{v}_c(k)$ only. The estimator uses measurements provided by the vehicle's sensors $\mathrm{y}_F(k) = [u(k), v(k), w(k), p(k), q(k), r(k)]^T$, and forces and moments provided by actuators as control inputs $\mathrm{u}_F(k) = \tau_a(k)$ that are estimated by actuators' models presented in the previous Section 2.

4. SIMULATION RESULTS

Reported results compare the OP facing a scenario featured by current disturbance with respect to the baseline OP neglecting the use of the TCE (OP_b). The MPC OP tuning parameters are collected in Table 2. Fig. 5 shows the comparison of OP trajectory, with respect to the OP_b in presence of the current ν_T featured by a speed of 0.514 m/s. The OP trajectory (black dashed line) is reported

Table 2. MPC tuning

Parameter	Symbol	Value	Units
Prediction horizon	N_p	5	-
Control horizon	N_u	3	-
OV weights	R	$diag([1,1])$	-
MV weights	Q	$diag([1,1,100])$	-
MV rates weights	P	$diag([10,10,1000])$	-
MV constraints	$u_{\max}$	4	m/s
	$u_{\min}$	-4	m/s
	$\psi_{\max}$	0.9	rad/s
	$\psi_{\min}$	0.9	rad/s
MV rate constraints	$\Delta u_{\max}$	1	m/s
	$\Delta u_{\min}$	-1	m/s
	$\Delta\psi_{\max}$	0.0873	rad/s
	$\Delta\psi_{\min}$	-0.0873	rad/s
Sampling time	T_s	0.1	s

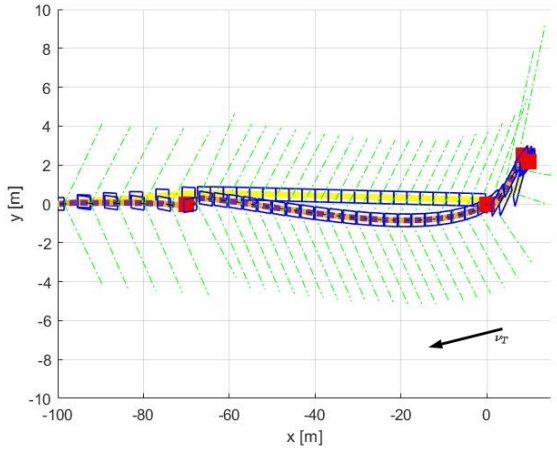

Fig. 5. Current-disturbed Test Results: OP-driven AUV trajectory (dashed blue plot) compared with baseline OP_b trajectory (yellow plot)

together with the AUV poses (blue shapes), way-points (red shapes) and sonar angular range (dashed green lines) whereas the OP_b trajectory is represented by the yellow line. Different trajectories are due to capability of OP to exploit TCE current estimation that is neglected in the OP_b. Estimated current velocities $\hat{v}_c$ and $\hat{u}_c$ used by the OP are shown in Fig. 6 (results reports 70 seconds of the test, because after WP0, the estimation is maintained constant to the last value, because current is constant and due to limited estimation capability during fast AUV maneuvering. The adapted trajectory permits to achieve a power consumption reduction of -7.85% by using the OP compared to the baseline OP_b. Further, a set of 100 Monte Carlo tests has been performed varying tidal current speed and direction, and docking station position and heading. This results permitted to achieve an average power consumption reduction of -5% by using OP compared to the OP_b policy performance.

5. CONCLUSIONS

A path planning algorithm has been presented for controlling an Autonomous Underwater Vehicle (AUV). The proposed approach involves several policies to generate trajectory way-points, to estimate the tidal current speed, and to construct the trajectory between way-points as a solution to an optimization problem. Results illustrated the ability of the proposed policy to adapt the path and limit power consumption. Future developments may consider alternative nonlinear optimization policies to improve the path planner performance (e.g. Nonlinear Model Predictive Control), and a study of the trade-off between computational complexity and control performance achievable by using different MPC paradigms.

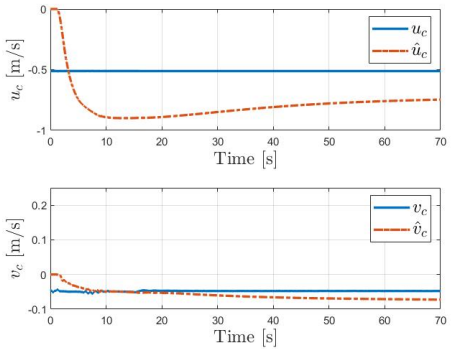

Fig. 6. Current-disturbed Test Results: Tidal Current Estimator Performance

REFERENCES

Albarakati, S., Lima, R.M., Giraldi, L., Hoteit, I., and Knio, O. (2019). Optimal 3d trajectory planning for auvs using ocean general circulation models. *Ocean Engineering*, 188, 106266.

Alvarez, A., Caiti, A., and Onken, R. (2004). Evolutionary path planning for autonomous underwater vehicles in a variable ocean. *IEEE Journal of Oceanic Engineering*, 29(2), 418–429.

Antonelli, G., Fossen, T.I., and Yoerger, D.R. (2016). Modeling and control of underwater robots. In *Springer Handbook of Robotics*, 1285–1306. Springer.

Cavanini, L. and Ippoliti, G. (2018). Fault tolerant model predictive control for an over-actuated vessel. *Ocean Engineering*, 160, 1–9.

Grimble, M.J. (2006). *Robust industrial control systems: optimal design approach for polynomial systems*. John Wiley & Sons.

Lewis, E.V. (1988). Principles of naval architecture second revision. *Jersey: Sname*, 2.

Medagoda, L. and Williams, S.B. (2012). Model predictive control of an autonomous underwater vehicle in an in situ estimated water current profile. In *2012 Oceans-Yeosu*, 1–8. IEEE.

Silvestre, C. and Pascoal, A. (2007). Depth control of the infante auv using gain-scheduled reduced order output feedback. *Control Engineering Practice*, 15(7), 883–895.

Zeng, Z., Lian, L., Sammut, K., He, F., Tang, Y., and Lammas, A. (2015). A survey on path planning for persistent autonomy of autonomous underwater vehicles. *Ocean Engineering*, 110, 303–313.

Zhu, D., Cao, X., Sun, B., and Luo, C. (2017). Biologically inspired self-organizing map applied to task assignment and path planning of an auv system. *IEEE Transactions on Cognitive and Developmental Systems*, 10(2), 304–313.